1-1-2013

Architecture designed ZnO hollow microspheres with wide-range visible-light photoresponses

Ziqi Sun
University of Wollongong, ziqi@uow.edu.au

Ting Liao
The University Of Queensland,University Of Queensland

Jae-Geun Kim
University of Wollongong, jgk884@uow.edu.au

KeSong Liu
University of Wollongong, kesong_liu@uow.edu.au

Lei Jiang
University of Wollongong

See next page for additional authors

Architecture designed ZnO hollow microspheres with wide-range visible-light photoresponses

Abstract

It is a challenge to increase the visible-light photoresponses of wide-gap metal oxides. In this study, we proposed a new strategy to enhance the visible-light photoresponses of wide-gap semiconductors by deliberately designing a multi-scale nanostructure with controlled architecture. Hollow ZnO microspheres with constituent units in the shape of one-dimensional (1D) nanowire networks, 2D nanosheet stacks, and 3D mesoporous nanoball blocks are synthesized via an approach of two-step assembly, where the oligomers or the constituent nanostructures with specially designed structures are first formed, and then further assembled into complex morphologies. Through deliberate designing of constituent architectures allowing multiple visible-light scattering, reflections, and dispersion inside the multiscale nanostructures, enhanced wide range visible-light photoresponses of the ZnO hollow microspheres were successfully achieved. Compared to the one-step synthesized ZnO hollow microspheres, where no nanostructured constituents were produced, the ZnO hollow microspheres with 2D nanosheet stacks presented a 50 times higher photocurrent in the visible-light range ($\lambda > 420$ nm). The nanostructure induced visible-light photoresponse enhancement gives a direction to the development of novel photosensitive materials.

Keywords

visible, range, wide, photoresponses, microspheres, light, hollow, zno, designed, architecture

Disciplines

Engineering | Physical Sciences and Mathematics

Publication Details

Sun, Z., Liao, T., Kim, J., Liu, K., Jiang, L., Kim, J. and Dou, S. X. (2013). Architecture designed ZnO hollow microspheres with wide-range visible-light photoresponses. Journal of Materials Chemistry C, (42 (September)), 6924-6929.

Authors

Ziqi Sun, Ting Liao, Jae-Geun Kim, KeSong Liu, Lei Jiang, Jung Ho Kim, and S X. Dou

Journal of Materials Chemistry C

Materials for optical and electronic devices

www.rsc.org/MaterialsC

Volume 1 | Number 42 | 14 November 2013 | Pages 6915–7118

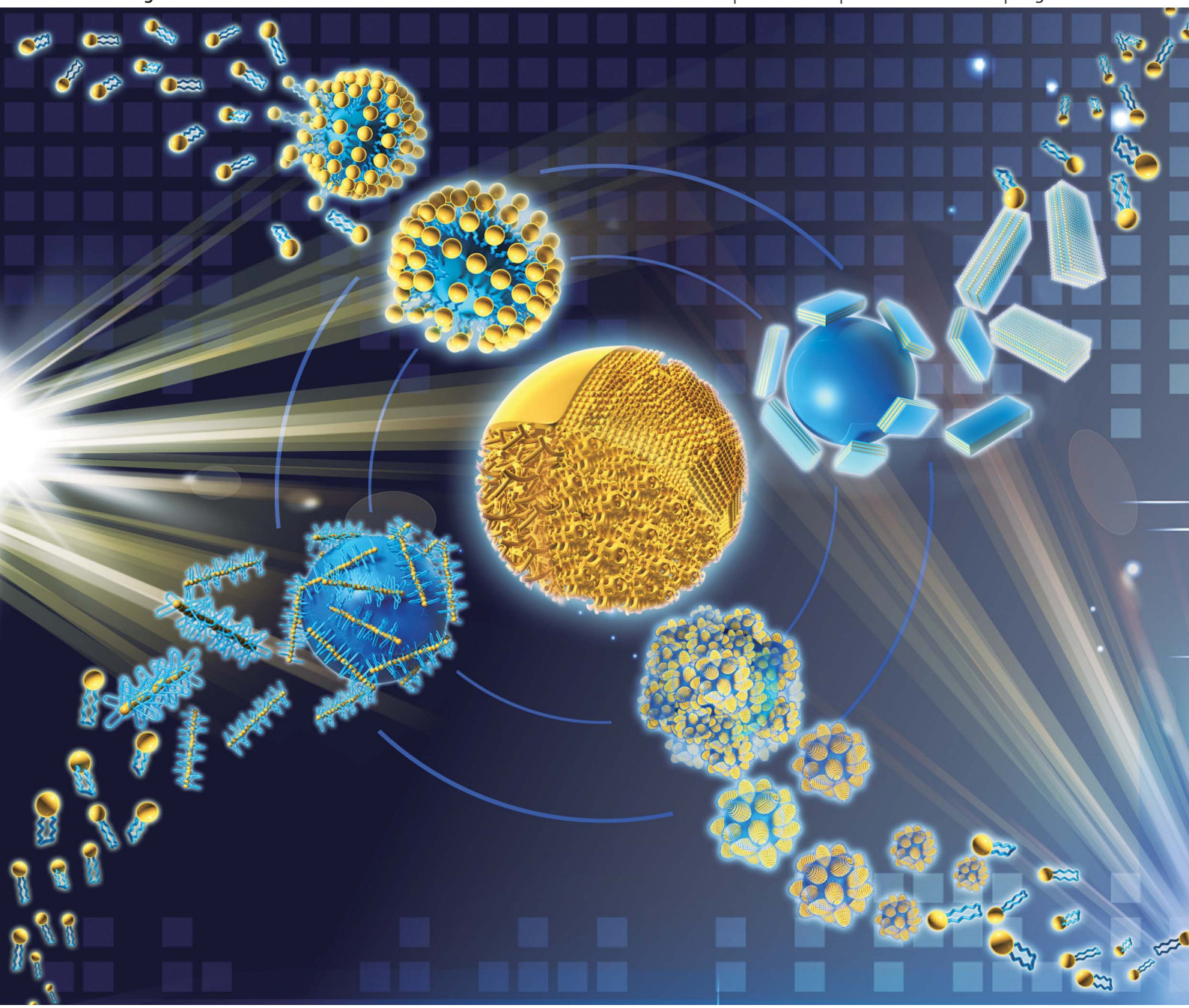

ISSN 2050-7526

RSC Publishing

COMMUNICATION

Kesong Liu, Jung Ho Kim *et al.*

Architecture designed ZnO hollow microspheres with wide-range visible-light photoresponses

2050-7526(2013)1:42;1-B

Journal of Materials Chemistry C

RSC Publishing

COMMUNICATION

View Article Online
View Journal | View Issue

Architecture designed ZnO hollow microspheres with wide-range visible-light photoresponses†

Cite this: *J. Mater. Chem. C*, 2013, **1**, 6924

Received 21st August 2013
Accepted 6th September 2013

DOI: 10.1039/c3tc31649a

www.rsc.org/MaterialsC

Ziqi Sun,[a] Ting Liao,[b] Jae-Geun Kim,[a] Kesong Liu,*[c] Lei Jiang,[cd] Jung Ho Kim*[a] and Shi Xue Dou[a]

It is a challenge to increase the visible-light photoresponses of wide-gap metal oxides. In this study, we proposed a new strategy to enhance the visible-light photoresponses of wide-gap semiconductors by deliberately designing a multi-scale nanostructure with controlled architecture. Hollow ZnO microspheres with constituent units in the shape of one-dimensional (1D) nanowire networks, 2D nanosheet stacks, and 3D mesoporous nanoball blocks are synthesized *via* an approach of two-step assembly, where the oligomers or the constituent nanostructures with specially designed structures are first formed, and then further assembled into complex morphologies. Through deliberate designing of constituent architectures allowing multiple visible-light scattering, reflections, and dispersion inside the multiscale nanostructures, enhanced wide range visible-light photoresponses of the ZnO hollow microspheres were successfully achieved. Compared to the one-step synthesized ZnO hollow microspheres, where no nanostructured constituents were produced, the ZnO hollow microspheres with 2D nanosheet stacks presented a 50 times higher photocurrent in the visible-light range (λ > 420 nm). The nanostructure induced visible-light photoresponse enhancement gives a direction to the development of novel photosensitive materials.

In recent years, an enormous amount of research has been devoted to the study of photosensitive materials, from both fundamental and practical viewpoints, due to their wide applications in photocatalytic and photoelectronic devices, ultraviolet (UV) detectors, photoswitch microdevices, light-emitting diodes, photovoltaic devices, and photoelectrochemical cells.[1–7] Metal oxides such as ZnO, TiO_2 and SnO_2 have been the most investigated photosensitive materials.[8–10] To enhance and take full advantage of the photosensitivity of metal oxides, a lot of strategies have been proposed to increase the photoresponses especially in the visible-light range, such as surface polymerization, light-element doping, or surface plasmon enhancement.[11–13] However, owing to the wide gap intrinsic to most metal oxides, it still remains a challenge to increase their visible-light photosensitivity. In this study, we will propose a new strategy to enhance the visible light photoresponses of wide-gap semiconductors by deliberately designing a multi-scale nanostructure with controlled constituent architectures.

Even though significant achievements have been made in the synthesis of isolated zero-, one-, and two-dimensional (0D, 1D, and 2D) nanostructures in the last decade, the well-controlled synthesis of complex nanostructures having both appropriately designed constituent nanostructures and well-defined overall shapes still remains a challenge.[14–17] Nanomaterials with complex structures can be tailored to meet certain functionalities that cannot be attained by the isolated and simple constituent nanostructures. For instance, three-dimensional (3D) hierarchical structures composed of 1D nanorod or nanowire units can provide improved photocatalytic activity, enhanced light harvesting, and superior electrochemical performance, because the salient structure simultaneously possesses low-dimensional 1D nanostructures and higher-order large-size aggregations. The multi-scale structures in the complex nanomaterials allow multiple light reflections and scattering, large surface area, and more reaction sites, as well as unique electronic transport and collection pathways, and thus much higher device performance.[18–21]

Herein, an approach of two-step self-assembly was employed to design multi-scale nanostructures of metal oxides, where the designed constituent oligomers or nanostructured units are

[a]*Institute for Superconducting and Electronic Materials, University of Wollongong, Innovation Campus, North Wollongong, NSW 2500, Australia. E-mail: jhk@uow.edu.au*

[b]*Australian Institute for Bioengineering and Nanotechnology, The University of Queensland, St Lucia, QLD 4072, Australia*

[c]*Key Laboratory of Bio-inspired Smart Interfacial Science and Technology of Ministry of Education, School of Chemistry and Environment, Beihang University, Beijing 100191, China. E-mail: liuks@buaa.edu.cn*

[d]*Beijing National Laboratory for Molecular Sciences (BNLMS), Key Laboratory of Organic Solids, Institute of Chemistry, Chinese Academy of Sciences, Beijing 100190, China*

† Electronic supplementary information (ESI) available: Synthesis method, SEM and TEM images of ZnO hollow microspheres, and photoresponse results. See DOI: 10.1039/c3tc31649a

first formed from structure-defined surfactant micelles, and then the desired architectural units are assembled into the final structure with the addition of a co-surfactant. Surfactant assisted self-assembly is a widely used method to synthesize diverse nanostructures and mesoporous structures, and is one of the easiest ways to control the morphology of nanostructures.[22–24] Scheme 1 presents a schematic diagram of our concept for the two-step self-assembly of complex nanostructures with specially designed 1D, 2D, and 3D building block architectures. Scheme 1(a) shows a traditional one-step self-assembly, where the precursors are assembled into the final shape directly. Scheme 1b and c show the two-step self-assembly, in which the oligomers or the nanostructured building units are first assembled into the designed structures, and then the constituent nanostructured units are self-organized into the final hollow spherical structures with the addition of a second co-surfactant. Based on this conceptual innovation, ZnO hollow microspheres with well-designed constituent units in the shapes of 1D nanowire networks, 2D nanosheet stacks, and 3D mesoporous nanoball blocks were successfully synthesized to meet the requirements of a high internal surface area and wide-range visible-light responses. Hollow spheres that were obtained *via* a one-step synthesis approach with the same starting solutions and synthesis conditions had solid smooth surfaces without any nanostructured constituents.

Fig. 1 shows the differences in the morphologies and constituent nanostructures of the ZnO hollow spheres that were synthesized *via* a traditional one-step approach (a–d) and the ones obtained *via* a deliberately designed two-step self-assembly method (e–p). The compositions of the precursor solution and the obtained morphologies are also listed in Table S1 in the ESI.†

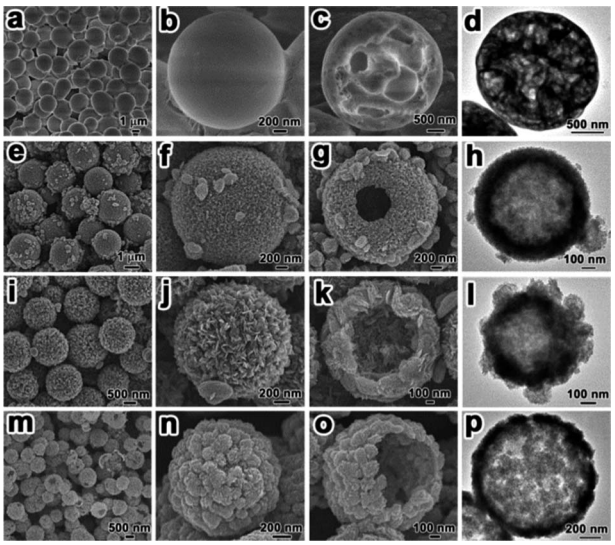

Fig. 1 Scanning and transmission electron microscopy (SEM and TEM) images of ZnO hollow microspheres synthesized by traditional one-step self-assembly (a–d), and two-step self-assembly by first organizing precursor oligomers into the shape of (e–h) continuous 1D nanowire networks, (i–l) 2D nanosheet stacks, and (m–p) 3D mesoporous nanoball blocks. The first column ((a), (e), (i) and (m)) contains the low magnification images, the second column ((b), (f), (j) and (n)) contains the high magnification images, the third column ((c), (g), (k) and (o)) displays the shell structures, and the fourth column presents TEM images of the ZnO hollow microspheres.

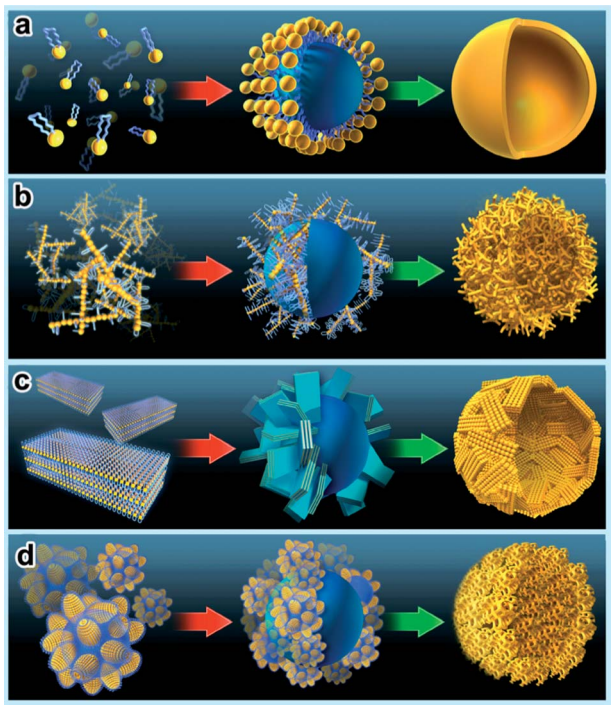

Scheme 1 Schematic diagram of synthesis of hollow microspheres *via* (a) a traditional one-step self-assembly, or (b–d) a two-step self-assembly approach, where the constituent nanostructures are first designed in the morphology of (b) continuous 1D nanowire networks, (c) 2D nanosheet stacks, and (d) 3D mesoporous nanoball blocks, and then assembled into the final hollow spherical structure.

Fig. 1(a)–(d) show the morphology of the ZnO hollow microspheres (ZHS-1) that were synthesized from solutions with all the chemicals added together, *i.e.* the normal one-step self-assembly, where the ratio of surfactant/water/alcohol was appropriate to form inverse spherical micelles (the solution composition in the area "B" of the phase diagram shown in Fig. S1†). The as-synthesized hollow microspheres have very smooth surfaces with an overall diameter of ~2.3 μm (Fig. 2(a)). Slightly increasing the precursor concentration (ZHS-1′) did not change the morphology, except for the bigger overall size (Fig. S2†). Fig. 1(e)–(h) and S3† present the morphology of the ZnO hollow spheres (ZHS-2) that were synthesized *via* a two-step self-assembly, where the constituent oligomers in the form of 1D nanowire networks were first formed from cubic micelles (area A in Fig. S1†), and the co-surfactant (or the oil-like phase) EG was then added to the solution to allow the further assembly of the nanostructured oligomers into hollow microspheres (area B in Fig. S1†). From the high magnification scanning electron microscope (SEM) images (Fig. 1(f) and (g)), we can see that the shells of the ZHS-2 hollow microspheres consist of well-defined nanowire networks and have a thickness of ~300 nm. Some nanowire network blocks of 200 nm size can also be clearly observed in Fig. S3.† Fig. 1(i)–(l) and S4† show the morphology of the hollow spheres (ZHS-3) synthesized from the solution with a higher surfactant/water ratio that is appropriate to form

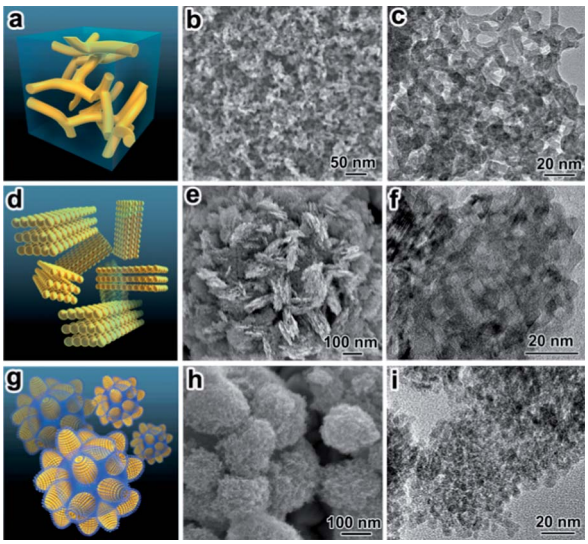

Fig. 2 Morphology of the constituent nanostructured units of ZnO hollow microspheres that were synthesized *via* the two-step assembly method: (a–c) schematic and high magnification images of the continuous 1D nanowire networks formed from cubic micelles, (d–f) schematic and high magnification images of the constituent 2D nanosheet stacks, and (g–i) schematic and high magnification images of the constituent 3D mesoporous nanoball blocks. (b), (e), and (h) are SEM images and (c), (f), and (i) are TEM images.

lamellar micelles. ZnO hollow spheres with shells in the form of 2D nanosheet stacks can be clearly observed. The synthesized hollow spheres were around 1.5 μm in size and had very homogeneous shapes (Fig. 1(i) and S4(a)†). The size of the nanosheet stacks was around 50 nm in thickness and 250–300 nm in width based on the SEM images in Fig. S4.† ZnO hollow microspheres with 3D mesoporous nanoball block constituents (ZHS-4) were obtained when we allowed sufficient self-assembly of the precursors by prolonging the aging time. The hollow microspheres around 1 μm in diameter that were finally assembled consisted of 3D mesoporous nanoball blocks of ~200 nm size, as shown in Fig. 1(m)–(p) and S5.† In this case, the shells of the ZnO hollow microspheres were not continuous 1D nanowire networks, but were formed from aggregated 3D mesoporous nanoball blocks.

The microstructures of the constituent 1D nanowire networks, 2D nanosheet stacks, and 3D mesoporous nanoball blocks of the two-step self-assembled ZnO hollow microspheres were further characterized using a high resolution SEM and transmission electron microscope (TEM) (Fig. 2 and S6–S8†). The shells of the ZnO hollow microspheres are found to consist of cross-linked nanowires with a diameter of around 10 nm (Fig. 2(b) and (c)). A high resolution TEM (HRTEM) image (Fig. S6†) shows that the nanowires themselves consist of wurtzite ZnO nanocrystallites ~5 nm in size. Fig. 2(c) shows a TEM image of the nanowire networks, which is in good agreement with the cubic mesoporous structure in the space group *Ia*3*d*. Fig. 2(d)–(f) demonstrates the structure and morphology of the 2D nanosheet stacks, which are usually stacks of 3–5 monolayers. Fig. S7–S8† present typical HRTEM images of the ZnO nanocrystallites in the 2D nanosheet constituent building blocks. The lattice fringes with distances of 2.8 Å coincide with the (010) and (010) planes of ZnO in the wurtzite phase. The XRD pattern also proves the wurtzite structure of ZnO (Fig. S9†). When there was sufficient hydrolysis of ZnO precursors, 3D mesoporous nanoball building blocks were obtained, as shown in Fig. 2(g)–(i). The corresponding SEM image demonstrates that the isolated nanoball blocks had a size of ~100 nm (Fig. 2(h)). The TEM image also shows that a mesoporous structure was formed inside the blocks (Fig. 2(i)). The HRTEM image (Fig. S10†) confirms the mesoporous structure of the 3D nanoball blocks with nanochannels of ~5 nm size inside.

In order to explore their applications as photocatalytic or photochromic materials, the specific surface areas of the ZnO hollow microspheres are extremely important. As shown in Fig. 3(a), the two-step self-assembled ZnO hollow microspheres showed improved specific surface areas (100–126 $m^2\ g^{-1}$) compared to the one-step assembly ones (38 $m^2\ g^{-1}$) and the single or multiple shelled ZnO hollow spheres reported by other authors (7–75 $m^2\ g^{-1}$).[25–27] The hollow spheres with shells composed of 2D nanosheet stacks (ZHS-3) reached a specific surface area of 126 $m^2\ g^{-1}$, which is almost two times higher than those of the reported single or multiple shelled ZnO hollow

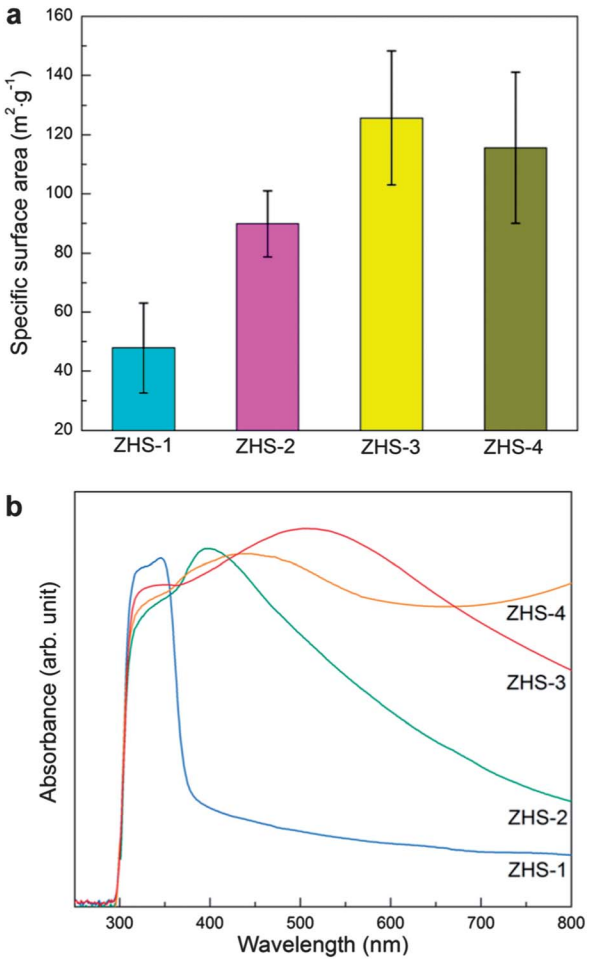

Fig. 3 (a) Specific surface areas of ZnO hollow microspheres and (b) UV-Vis absorbance spectra of ZnO hollow microspheres.

spheres and aerogel-like ZnO hierarchical structures.[25–27] The superior specific surface areas of the two-step assembled ZnO hollow microspheres are contributed by the well-designed multi-scale nanostructures, which should be helpful to enhance chemical adsorptions and improve surface chemical reaction sites.

To explore the effect of constituent architectures on the photoresponses of ZnO hollow microsphere photoelectrodes, the ultraviolet-visible (UV-Vis) light absorbance over the range 250–800 nm was tested. Fig. 3(b) presents the UV-Vis absorbance spectra of the ZnO hollow spheres in the wavelength range of 250–800 nm. For the one-step self-assembled hollow spheres with smooth surfaces (ZHS-1), the absorbance onset edge was around 370 nm, corresponding to a band gap of 3.35 eV, which coincides well with the band gap of nanosized ZnO.[28] The absorbance onset edges in the UV region for the two-step self-assembled hollow spheres with nanowire network, nanosheet stack, nanoball block constituents (ZHS-2,-3,-4), however, were overlapped by the visible light absorption. Two absorption peaks were distinguished in the spectra of ZHS-2,-3,-4. The first one in the UV range that has a similar position to that of ZHS-1 should be assigned to the absorption of the intrinsic band edge of the nanosized ZnO. The second peak in the visible light regime (400–750 nm) was attributed to strong visible-light absorbance. This strong visible light absorbance should be attributed to the multiple light scatterings, reflections, refractions, and dispersions by the micro-sized hollow spheres together with the complex constituents of nanowire networks, nanosheet stacks, or mesoporous nanoball blocks (Fig. S11†). These multiple optical effects have been successfully employed to enhance the visible-light harvesting capability of solar energy harvesting devices.[29–31] It is interesting that the visible light absorption of the ZnO hollow microspheres has strong correlation with the size of the constituent nanostructured aggregates. In detail, the visible light absorption centre of the hollow microspheres shifted from 400 nm to 450 nm and then to around 510 nm, with the variation of the constituent nano-units from nanowire network (~200 nm), to mesoporous nanoballs (~200 nm), and then to nanosheet stacks (250–300 nm in width). Thus, the two-step self-assembled ZnO hollow microspheres with superior features of both high-specific surface area and strong visible-light absorption could be promising candidate materials for superior photosensitive devices.

Fig. 4 shows the photoresponse behaviour of the integrated ZnO hollow microsphere photoelectrodes under alternating visible-light (λ > 420 nm, 65 mW cm^{-2}) and dark illumination (Fig. 4(a)), alternating simulated solar light (100 mW cm^{-2}) and visible light (Fig. 4(c)), as well as alternating 325 nm UV irradiation (15 mW cm^{-2}) and dark (Fig. 4(d)), at 1 V bias and 10 s interval. The active area of the electrodes under irradiation is 1 cm^2 by applying a black mask. In this study, the electrodes that have the morphologies of a smooth surface (ZHS-1), 1D nanowire networks (ZHS-2), 2D nanosheet stacks (ZHS-3), and 3D mesoporous nanoballs (ZHS-4) were subjected to photosensitivity testing. Due to the significant visible-light absorption in ZHS-3 and ZHS-4, as shown in Fig. 4(a), these materials

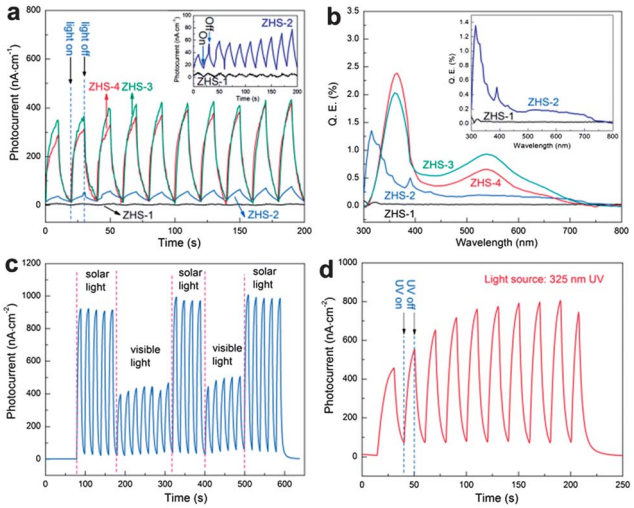

Fig. 4 (a) Visible-light photoresponses of ZnO hollow microsphere electrodes with 1 cm^2 active area with the morphology of a smooth surface (ZHS-1), 1D nanowire networks (ZHS-2), 2D naonsheet stacks (ZHS-3), and 3D mesoporous nanoballs (ZHS-4), under alternating visible-light (λ > 420 nm, 65 mW cm^{-2}) and dark illumination at 1 V bias and 10 s interval, the inset shows the photocurrent of ZHS-1 and ZHS-2; (b) the corresponding quantum emission efficiency in the range 300–800 nm, the inset shows the quantum efficiency of ZHS-1 and ZHS-2; (c) the photoresponse behaviour of the ZnO hollow microspheres (ZHS-3) under alternating simulated solar light (100 mW cm^{-2}) and visible light illuminations at 1 V bias and 10 s interval; and (d) the photoresponse behaviour of ZHS-3 under alternating UV light (325 nm, 15 mW cm^{-2}) and dark illumination.

presented a much higher photocurrent (~400 nA cm^{-2}) under visible-light irradiation than that of ZHS-1 (~8 nA cm^{-2}) and ZHS-2 (~80 nA cm^{-2}). It corresponds to a 50 times enhancement in the sensitivity of the photoelectrodes to visible light. Fig. 4(b) presents the quantum emission efficiency of the photoelectrodes in the range of 300–800 nm. It shows that the electrodes with nanosheet and mesoporous nanoball constituents had significant visible-light quantum emission, while the ZnO hollow microspheres without secondary nanostructures almost had no visible-light photoresponses. The significant visible light absorption of the ZHS with fine nanostructures confirmed the importance of the secondary nanostructures in the photoresponses of photosensitive materials. The visible light–photocurrent responses of the two-step synthesized ZnO_2 hollow microspheres might be contributed by the following factors: (i) the hierarchical orders of the nanostructured constituent units and microsized hollow spheres result in significant multiple scattering, reflection, refraction, and dispersion, which increase the transport path of light within the hollow microspheres, (ii) the fine nanostructures dramatically increase not only the specific surface area but also the photon trapping centres such as nanosized holes, edges, arms, and ordered channels, and (iii) the possible existence of a superficial dipole layer formed as a result of the residual surfactant molecules, which has been demonstrated to have a great influence on the spectroscopic properties of nanocrystallites.[32–34] Fig. 4(c) presents the photoresponse behaviour of the ZnO hollow microspheres, with ZHS-4 as an example, under alternating simulated solar light and visible light,

demonstrating the difference in photoresponses under the full-spectrum solar light and visible light. The photocurrent and photoresistance of ZHS-2 under alternating solar light and visible light illumination are presented in Fig. S12(a) and (b).† The higher photocurrent under solar light illumination correlates with the lower resistance of the photoelectrode, which means a higher concentration of charge carriers under solar light including UV irradiation. The photoresponse of ZHS-4 under UV irradiation at 325 nm is also shown in Fig. 4(d). It shows that the photocurrent increased stepwise in the initial few on–off cycles, due to the continuous increase of the carrier concentration under UV until saturation. This phenomenon can be explained by the "light soaking" effect, which has been observed in the photoanodes made from wide band-gap metal oxides, such as SnO_2, TiO_2, *etc.*[35–37] The light soaking effect of UV can be observed not only in charge generation but also in the charge decay after light switch-off. Both the response time and recovery time of charge transport under visible-light irradiation were over 30 s (Fig. S12(c)†). This process, however, is much faster in the samples under UV irradiation. Fig. S12(d)† presents the decay curves of the photocurrents of ZHS-4 after irradiating under UV light and solar light. The decay time is much longer for the visible light irradiated samples (~170 s) compared to that of the UV irradiated samples (~10 s), indicating the rapid charge transport in the UV irradiated samples.

Conclusions

In summary, ZnO hollow microspheres with different visible light photoresponses were synthesized by deliberate tailoring of the constituent architectures. Through the deliberate designing of constituent architectures that allow multiple visible-light scattering, reflection, refraction, and dispersion inside the multi-scale hollow microspheres, as well as produce a high density of photon trapping centres such as nanosized holes, edges, arms, and ordered channels, enhanced wide range visible-light photoresponses of the ZnO hollow microspheres were successfully achieved. Compared to the one-step synthesized ZnO hollow microspheres, where no nanostructured constituents were produced and the visible-light photocurrent was only ~8 nA cm^{-2}, the ZnO hollow microspheres with 2D nanosheet stacks presented a 50 times higher photocurrent in the visible-light range (λ > 420 nm) with a photocurrent of ~400 nA cm^{-2}. The nanostructure induced visible-light photoresponse enhancement gives a direction to develop novel photosensitive materials.

Acknowledgements

This work was supported by Australian Research Council Discovery Project DP1096546, the National Natural Science Foundation of China (21273016 and 21001013), the National Basic Research Program of China (2013CB933003), the Program for New Century Excellent Talents in Universities, Beijing Natural Science Foundation (2122035). ZQS was supported by an ARC Postdoctoral (APD) Research Fellowship and a UOW Vice-Chancellor's (VC) Research Fellowship. TL was supported by a UQ Postdoctoral Research Fellowship.

Notes and references

1 S. Yang, H. Ma, Y. Luo and J. Gong, *ChemPhysChem*, 2012, **13**, 2289.
2 N. Tétreault and M. Grätzel, *Energy Environ. Sci.*, 2012, **5**, 8506.
3 B. K. Pathem, S. A. Claridge, Y. B. Zheng and P. S. Weiss, *Annu. Rev. Phys. Chem.*, 2013, **64**, 605.
4 T. Alammar and A. Mudring, *ChemSusChem*, 2011, **4**, 1796.
5 A. Kolmakov and M. Moskovits, *Annu. Rev. Mater. Res.*, 2004, **34**, 151.
6 A. J. Nozik, *Nano Lett.*, 2010, **10**, 2736.
7 K. Shankar, J. I. Basham, N. K. Allam, O. K. Varghese, G. K. Mor, X. Feng, M. Paulose, J. A. Seabold, K. Choi and C. A. Grimes, *J. Phys. Chem. C*, 2009, **113**, 6327.
8 I. Gonzalez-Valls and M. Lira-Cantu, *Energy Environ. Sci.*, 2009, **2**, 19.
9 M. Ni, M. K. H. Leung, D. Y. C. Leung and K. Sumathy, *Renewable Sustainable Energy Rev.*, 2007, **11**, 401.
10 M. Shimura, K. Shaushiro and Y. Shimura, *J. Appl. Electrochem.*, 1986, **16**, 683.
11 C. S. Lao, M. C. Park, Q. Kuang, Y. L. Deng, A. K. Sood, P. L. Polla and Z. L. Wang, *J. Am. Chem. Soc.*, 2007, **129**, 12096.
12 G. Liu, L. Yin, J. Wang, P. Niu, C. Zhen, Y. Xie and H. M. Cheng, *Energy Environ. Sci.*, 2012, **5**, 9603.
13 S. S. K. Ma, K. Maeda, R. Abe and K. Domen, *Energy Environ. Sci.*, 2012, **5**, 8390.
14 J. N. Tiwari, R. N. Tiwari and K. S. Kim, *Prog. Mater. Sci.*, 2012, **57**, 724.
15 X. Li, X. Wang and M. Antonietti, *Chem. Sci.*, 2012, **3**, 2170.
16 Q. H. Wang, K. Kalntar-Zadeh, A. Kis, J. N. Coleman and M. S. Strano, *Nat. Nanotechnol.*, 2012, **7**, 699.
17 Z. Sun, J. H. Kim, Y. Zhao, F. Bijarbooneh, V. Malgras and S. X. Dou, *CrystEngComm*, 2012, **14**, 5472.
18 J. H. Pan, X. Zhang, A. J. Du, D. D. Sun and J. O. Leckie, *J. Am. Chem. Soc.*, 2008, **130**, 11256.
19 Z. Sun, J. Kim, Y. Zhao, F. Bijarbooneh, V. Malgras, Y. Lee, Y. M. Kang and S. X. Dou, *J. Am. Chem. Soc.*, 2011, **133**, 19314.
20 Z. Sun, J. H. Kim, Y. Zhao, D. Attard and S. X. Dou, *Chem. Commun.*, 2013, **49**, 966.
21 P. Yang, *MRS Bull.*, 2012, **37**, 806.
22 J. Vivero-Escoto, Y. Chiang, K. Wu and Y. Yamauchi, *Sci. Technol. Adv. Mater.*, 2012, **13**, 013003.
23 N. Suzuki, X. Jiang, L. Radhakrishnan, K. Takai, K. Shimasaki, Y. Huang, N. Miyamoto and Y. Yamauchi, *Bull. Chem. Soc. Jpn.*, 2011, **84**, 812.
24 H. Oveisi, A. Beitollahi, X. Jiang, K. Sato, Y. Nemoto, N. Fukuta and Y. Yamauchi, *J. Nanosci. Nanotechnol.*, 2011, **11**, 6926.
25 Z. Dong, X. Lai, J. E. Halpert, N. Yang, L. Yi, J. Zhai, D. Wang, Z. Tang and L. Jiang, *Adv. Mater.*, 2012, **24**, 1046.
26 S. Dilger, C. Lizandara-Pueyo, M. Krumm and S. Polarz, *Adv. Mater.*, 2012, **24**, 543.

27 J. Yu and X. Yu, *Environ. Sci. Technol.*, 2008, **42**, 4902.
28 F. Xu and L. Sun, *Energy Environ. Sci.*, 2011, **4**, 818.
29 W. Shao, F. Gu, L. Gai and C. Li, *Chem. Commun.*, 2011, **47**, 5046.
30 S. Ito, S. M. Zakeeruddin, R. Humphty-Baker, P. Liska and R. Charvet, *Adv. Mater.*, 2006, **18**, 1202.
31 Z. Sun, J. H. Kim, Y. Zhao, F. Bijarbooneh, V. Malgras and S. X. Dou, *J. Mater. Chem.*, 2012, **22**, 11711.
32 S. Leung, M. Yu, Q. Lin, K. Kwon, K. Ching, L. Gu, K. Yu and Z. Fan, *Nano Lett.*, 2012, **12**, 3682.
33 F. Flory, L. Escoubas and G. Berginc, *J. Nanophotonics*, 2011, 052502.
34 B. Yu, C. Zhu and F. Gan, *Opt. Mater.*, 1997, **7**, 15.
35 P. Tiwana, P. Docampo, M. B. Johnston, L. M. Herz and H. J. Snaith, *Energy Environ. Sci.*, 2012, **5**, 9566.
36 Q. Wang, Z. Zhang, S. M. Zakeeruddin and M. Gratzel, *J. Phys. Chem. C*, 2008, **112**, 7084.
37 A. Listorti, C. Creager, P. Sommeling, J. Kroon, E. Palomares, A. Fornelli, B. Breen, P. R. F. Barnes, J. R. Durrant, C. Law and B. O'Regan, *Energy Environ. Sci.*, 2011, **4**, 3494.